# Mixture effects in alkane/cycloalkane hydroconversion over Pt/HUSY : carbon number impact

Nebojsa Korica [a], Arij Ben Hassine [b], Hang Dao Thi [a], Latifa Bergaoui [b], Kevin M. Van Geem [a], Pedro S.F. Mendes [a $], Jeriffa De Clercq [c], and Joris W. Thybaut * [a]

[a] Laboratory for Chemical Technology, Ghent University, Technologiepark 125, B-9052 Ghent, Belgium

[b] EcoChimie Laboratory, National Institute of Applied Science and Technology, Carthage University, Centre Urbain Nord BP 676, 1080 Tunis, Tunisia

[c] Industrial Adsorption and Catalysis Technology, Ghent University, Valentin Vaerwyckweg 1, B-9000 Ghent, Belgium

* Corresponding author, e-mail: Joris.Thybaut@UGent.be

[$] Present address: Centro de Química Estrutural, Instituto Superior Técnico, Universidade de Lisboa, Av. Rovisco Pais, 1049-001 Lisbon, Portugal

*Abstract*

Cycloalkanes are known to impact the metal-acid balance of the hydrocracking of *n*-alkanes with similar carbon number, however, how this impact varies with the carbon number of the components involved is still to be understood in more detail. For this purpose, the hydroconversion of *n*-octane and tert-butylcyclohexane, and *n*-decane and methylcyclohexane mixtures was investigated in this work over Pt/HUSY catalyst in both the ideal and the nonideal hydrocracking regime. Irrespective of the hydrocracking regime for pure *n*-octane, its conversion and isomer yields were significantly lowered upon admixture of tert-butylcyclohexane. On the other hand, *n*-octane admixture did not impact the tert-butylcyclohexane conversion nor its cyclic isomer yields. Upon methylcyclohexane admixture with *n*-decane, no impact was observed over the catalyst ensuring ideal hydrocracking of pure *n*-decane. Over the catalyst with significantly lower Pt loading, which does not ensure ideal hydrocracking of *n*-decane,

methylcyclohexane lowered the *n*-decane conversion. A slightly negative impact of *n*-decane admixture on methylcyclohexane conversion was also observed. The observed effects are mainly attributed to the differences in adsorption strengths within the zeolite pores on top of differences in alkane and cycloalkane adsorption on the metal sites.

## *Highlights*

- *n*-Alkane hydrocracking is more negatively impacted with admixture of heavier cycloalkanes.
- Cycloalkane adsorbs on metal sites more favorably than *n*-alkane with higher carbon number.
- Larger alkanes impact cycloalkanes conversion only by preferred physisorption.

Key words : hydrocracking; carbon number impact; dehydrogenation; protonation; physisorption

## *1. Introduction*

Hydroconversion (hydroisomerization and -cracking) is one of the important conventional conversion processes for the production of different oil based products[1-3]. Despites its origin in the refining of fossil resources, this process remains crucial and even has a bright future for the rearrangement of hydrocarbon molecules in the continuously evolving context of stricter environmental policies and tendencies towards renewable fuels and chemicals. Hydroconversion feedstocks are, generally, complex mixtures of alkanes, cycloalkanes, aromatic, and heterocyclic compounds, etc[1-4]. As hydroconversion units are usually preceded by hydrotreating units, where unsaturated, aromatic, and heterocyclic components are saturated, alkanes and cycloalkanes represent the main components fed to a hydroconversion reactor[1, 2].

The hydroconversion of alkanes and cycloalkanes is catalyzed by a bifunctional catalyst, which contains metal and acid (Brønsted) active sites and, as indicated by the name, occurs under a hydrogen atmosphere[4-7]. The hydroconversion mechanism is shown in Figure 1. After physisorption of the reacting species in the pores of the catalyst, c.q., zeolite, unsaturated hydrocarbons are formed by dehydrogenation on metal active sites[4-6, 8, 9]. Subsequently, these intermediate products are protonated on Brønsted sites, forming (cyclo)alkyl-carbenium ions[10, 11]. The protonated species react in elementary

isomerization (hydride-, alkyl-shifts, and protonated-cyclopropane (PCP) branching) or cracking (β-scission) reactions[4, 7, 10, 12]. The cycloalkyl-carbenium ions can undergo elementary reactions within the ring structure and in the aliphatic part of the molecule. In addition to the above mentioned reaction families for aliphatic hydrocarbons, cycloalkanes undergo ring isomerization (intra-ring alkyl shifts and cyclic PCP branching), dealkylation (exocyclic), and ring opening (endocyclic β-scission) reactions[13, 14]. Reaction rates decrease from alkyl-shifts, PCP branching to β-scission, indicating that isomers are primary products, while cracking products are secondary[10, 12, 13, 15].

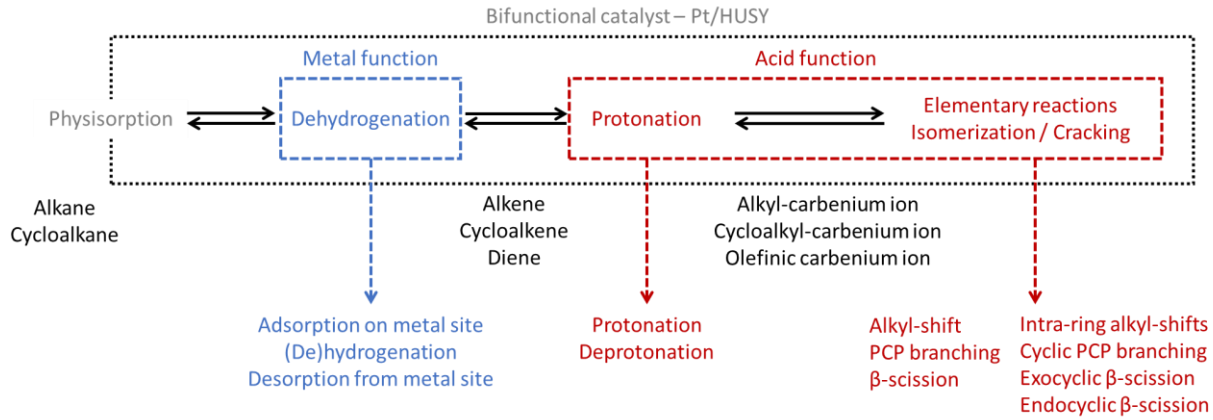


**Figure 1 Hydroconversion mechanism over bifunctional catalyst[16]**

When the product yields of the overall hydroconversion solely depend on the kinetics of elementary reactions catalyzed by the acid sites, the specific reaction regime is denoted as 'ideal hydrocracking'[4, 10]. This situation occurs when (de)hydrogenation reactions on metal active sites are quasi-equilibrated and, in that way, consecutive transformations of protonated species are avoided[4, 7], i.e., within a catalytic cycle starting and ending with saturated components, only a single acid-catalyzed rearrangement or cracking step has occurred. The equilibration of the (de)hydrogenation reactions is ensured by a sufficiently high ratio of metal to acid sites and the operating conditions. Furthermore, the intimacy between metal and Brønsted acid sites should be adequate to avoid any impact of mass transfer limitations on the ideality of the hydroconversion[7, 17-23]. On the other hand, increasing the acid sites concentration or decreasing the metal sites concentration will lead to a reaction regime in which both (de)hydrogenation and acid-

67 catalyzed reactions become kinetically relevant, also denoted as 'nonideal hydrocracking'[4, 7, 10]. On such a
68 catalyst or at such operating conditions, the overall hydroconversion rate is lowered and consecutive
69 reactions on acid sites are more likely to occur leading to higher selectivities towards higher order
70 products, such as more highly branched isomers and, particularly, cracking products[4, 17, 18]. In addition to
71 the ratio of metal to acid sites and their intimacy, reaction conditions impact the occurrence of ideal
72 hydrocracking[24]. With higher temperature, higher hydrogen-to-hydrocarbon ratio, and higher reactant
73 carbon number, a larger concentration of metal sites is required to maintain ideal hydrocracking[24]. In
74 contrast, a higher total pressure has a positive impact on the (de)hydrogenation reactions inducing a shift
75 from nonideal to ideal hydrocracking[24]. Besides the mentioned properties, establishing quasi-equilibrium
76 for the (de)hydrogenation reaction depends on the feedstock composition as well[16].
77 The generic impact of cycloalkane admixture on the hydrocracking mechanism and, consequently on the
78 ideal hydrocracking occurrence, is not well studied yet. Nevertheless, some specific aspects related to the
79 cycloalkane admixture impact on alkane hydroconversion were reported. A negative impact of cycloalkane
80 admixture on alkane hydroconversion was reported by Sanchez et al.[25], Jimenez et al.[26], Roldan et al.[27],
81 Hollo et al.[28], and Guisnet and Fouche[29]. The cycloalkane admixture impact in combination with shape
82 selectivity in zeolites lead to an increased amount of cracking products[26-28]. Finally, in our previous work,
83 the impact of methylcycloalkane admixture on *n*-octane hydrocracking over Pt/HUSY catalyst was
84 thoroughly investigated as a function of the "metal-acid balance"[16]. To limit the impact of carbon number,
85 two reagents (*n*-octane and methylcyclohexane) of similar physico-chemical properties were used.
86 Methylcyclohexane admixture decreased the *n*-octane conversion and isomer yield, especially over poorly-
87 balanced catalysts, i.e., the ones which could not ensure ideal hydrocracking of pure *n*-octane. In contrast,
88 *n*-octane admixture changed neither methylcyclohexane conversion nor cyclic isomers selectivity.
89 Apparently, methylcyclohexane lowers the effective ratio of metal over acid sites available for *n*-octane
90 hydrocracking, inducing a shift from ideal to nonideal hydrocracking. This methylcyclohexane admixture

impact was attributed to preferential adsorption on metal sites, which was believed to be a consequence of the molecule configuration[16]. Nevertheless, the impact of the carbon number of molecules in the mixture on this conclusion has not yet been systematically assessed. The admixture may be reinforced or weakened for molecules with different physico-chemical properties. Therefore, investigating the impact of the carbon number of reacting molecules completes these prior observations and conclusions.

The physisorption of saturated hydrocarbons on the zeolite surface is stronger with increased carbon number[30-33]. Correspondingly, stronger adsorption on the metal sites could be expected for components with a higher carbon number in comparison to *n*-octane. Furthermore, for alkanes below carbon number 10 the protonation enthalpy (slightly) becomes less negative with decreasing carbon number[10]. In addition to the adsorption properties, the chemical reactivity of components on the acid sites increases with the carbon number due to more extensive elementary reaction network[12, 13, 24]. For instance, among others due to entropic limitations of ring opening reactions, the methylcyclohexane reaction network was limited only to isomerization to four isomers[16] (Figure 2), while the reaction network of the larger tert-butylcyclohexane is about a hundred times more extensive, containing not only isomerization, but also dealkylation reactions. (Figure 3 shows examples of possible tert-butylcyclohexane reactions). Hence, investigation of the carbon number impact is necessary to gain a realistic insight in cycloalkane admixture effect on alkane hydroconversion. Monteiro et al. proposed a mechanism for cycloalkane hydroconversion which includes direct formation of carbenium ion via protolytic cracking, while the formed unsaturated products are hydrogenated on metal sites[34]. Cycloalkane hydroconversion could perhaps occur via the mechanism proposed by Monteiro et al.[34], but only in parallel with the classical bifunctional mechanism involving reactant dehydrogenation. As in our recent work[16] no deviations from the classic mechanism displayed Figure 1 could be identified, it was also used in this work (Figure 2 and 3).

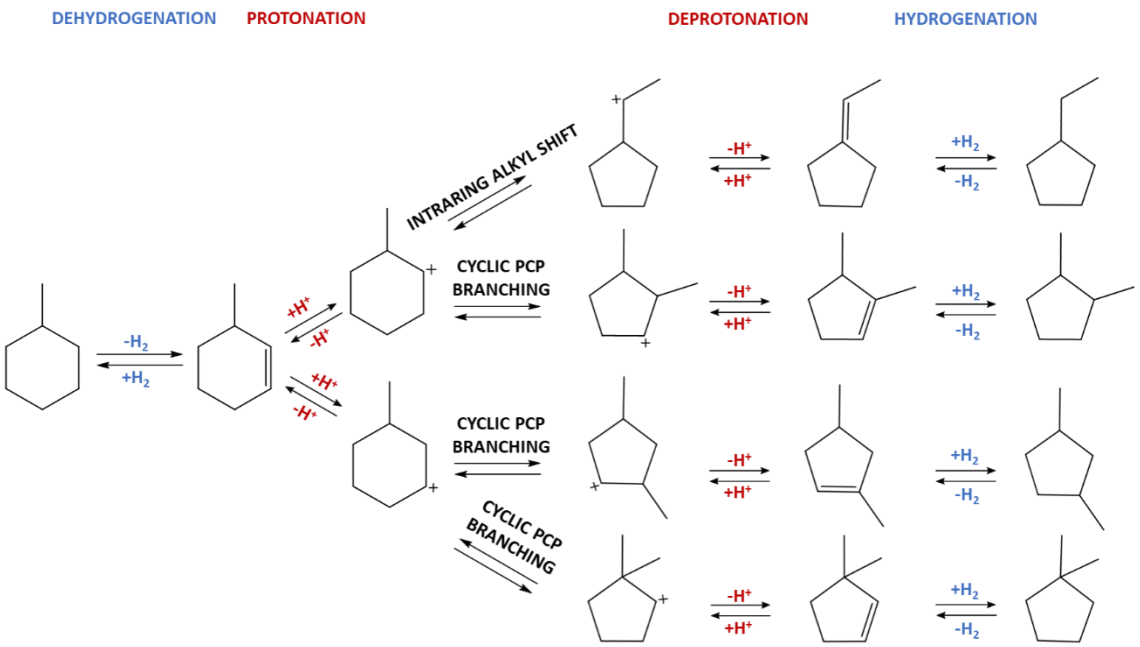


**Figure 2 Hydroconversion reaction network of methylcyclohexane inside the zeolite pores**

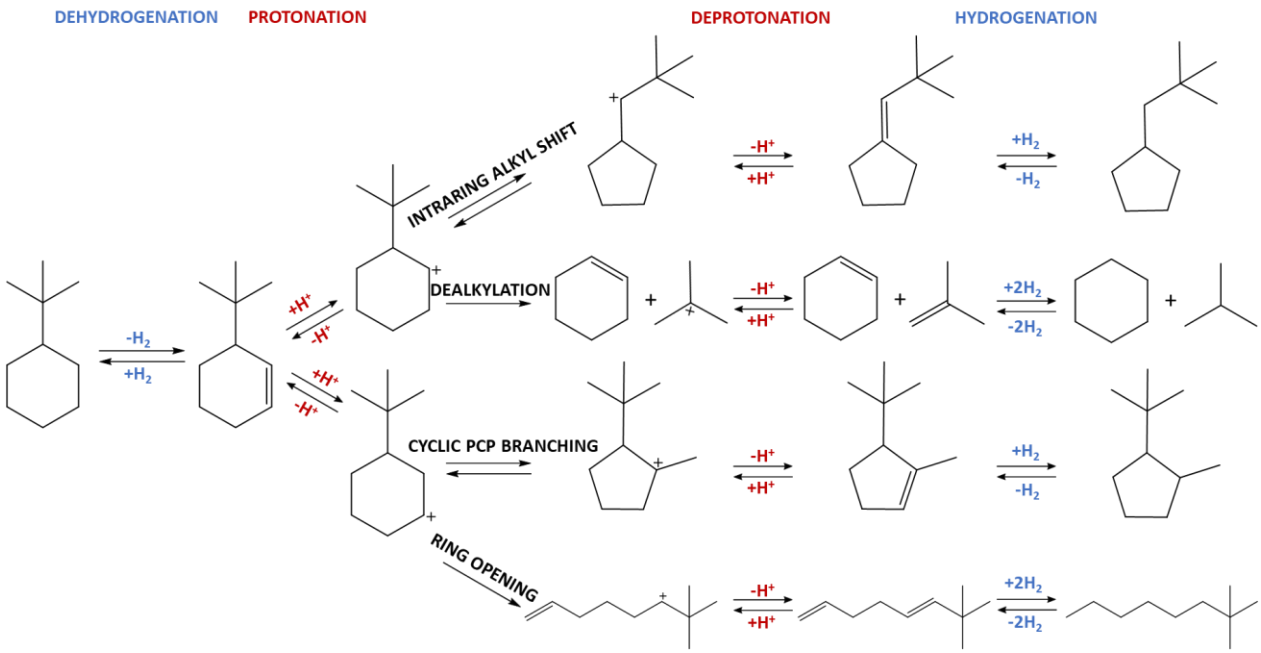


**Figure 3 Examples of hydroconversion routes of tert-butylcyclohexane inside the zeolite pores**

The assessment of the carbon number impact, and hence, of the differences in physico-chemical characteristics of the alkane and the cycloalkane, on their admixture is the aim of this work. In order to keep those differences in a comparable range and to further build on our previous work[16] *n*-octane and *n*-

decane, as alkane, and methylcyclohexane and tert-butylcyclohexane as cycloalkane model components were selected. This ensures reliable comparison of admixture effects and fundamental understanding which can be extrapolated for any carbon number. As the ratio of metal to acid site represents the key parameter for the occurrence of ideal hydrocracking, catalysts with different metal to acid sites ratios were examined with all the above mentioned model components. In order to have sufficient strong acid sites and to avoid shape selectivity, Pt/USY catalysts with significant mesoporosity were used.

## 2. *Materials and methods*

### *2.1. Catalyst synthesis*

Zeolite HUSY (CBV712 with molar $SiO_2/Al_2O_3$ ratio of 12, supplied by Zeolyst), was loaded with Pt via incipient wetness impregnation[35, 36] to obtain three different catalysts: 0.3 wt%Pt/HUSY; 0.1 wt%Pt/HUSY; and 0.07 wt%Pt/HUSY (Table 1). Tetraammineplatinum(II)-nitrate hexahydrate $[Pt(NH_3)_4(NO_3)_2]\cdot 6H_2O$ (Sigma Aldrich 99.995%) was used as Pt precursor. After impregnation, the catalysts were dried overnight in an oven at 393 K. The catalysts were subsequently calcined under static air in an oven (Nabertherm P330) according to a stepwise temperature program: three plateaus at 423, 523, and 623 K for 1 h, and one plateau at 773 K for 2 h with a 5 K/min heating rate to each plateau (see Supporting information Figure S1).

### *2.2. Catalyst characterization*

The specific surface area of the catalysts was determined via $N_2$ adsorption on a TriStar II device (Micromeritics) using the t-plot method (see Supporting information Section S2). The elemental analysis of the catalysts was determined with Inductively Coupled Plasma-Optical Emission Spectrometry (ICP-OES, IRIS intrepid II XSP from Thermo Scientific) (Table 1 and Supporting information Section S3).

The Pt reduction was investigated by hydrogen temperature programmed reduction ($H_2$-TPR) in an Autochem II 2920 device (Micromeritics) with a thermal conductivity detector. The reduction profiles are shown in Figure S2 in Supporting Information Section S4. The samples (about 0.3 g) were heated up to 873

K for 1 h under a gas (5% $H_2$ in Ar) flow of 0.17 Nml/s. The degree of Pt reduction was determined based on the volume of consumed hydrogen and platinum content determined by ICP-OES[36] (Table 1 and Supporting information Section S4).

The Pt dispersion was determined by hydrogen-oxygen titration[35-38] in an Autochem II 2920 device (Micromeritics) with a thermal conductivity detector (TCD). The samples (0.2 - 0.3 g) were initially pretreated under $H_2$ at 473 K for 30 min and at 723 K for 60 min. Subsequently the samples were cooled to 308 K and consecutive pulses of $H_2$ were injected with an interval of 3 min until no further adsorption was observed. After purging with He for 45 min, consecutive $O_2$ pulses (with intervals of 3 min) were injected until no further adsorption was observed. The samples were purged with Ar for 45 min and then $H_2$ pulses were injected. Another cycle of oxygen and hydrogen titration was performed in order to ensure repeatability. A stoichiometric factor (Pt:$H_2$) of 0.67 is used for the calculation of the Pt dispersion[38] (see Supporting information Section S5).

The Pt dispersion was assessed via transmission electron microscopy (TEM). The dark field scanning transmission electron microscopy (STEM DF) in a JEM-2200FS Cs corrected microscope device (JEOL) operated at 200kV with Schottky type field emission gun (FEG) and EDX was used. The samples were deposited on a lacey carbon film with a copper grid support. The average particle size did not significantly deviate from 1 nm for all catalysts (Table 1). Representative TEM images with particle size distributions are enclosed in Supporting information Section S6.

Ammonia temperature programmed desorption ($NH_3$-TPD) to determine the catalysts acidity was performed in an AutoChem 2920 device (Micromeritics). The samples (0.1 – 0.15 g) were pretreated under a constant He flow rate of 1 NmL/s, by heating to 873 K (with a heating rate 20 K/min) and cooling back to 373 K. The gas flow was changed to 4 vol% $NH_3$-He with a flow rate of 1 Nml/s for 1 h. Finally, the sample was heated to 873 K for 50 min under a constant He flow, and the amount of ammonia desorbed was recorded using a thermal conductivity detector. $NH_3$-TPD profiles of the catalysts and pure HUSY were not

significantly different. This shows that the acidity was not significantly impacted by the Pt loading (Table 1 and Supporting information Section S7).

The Brønsted acid sites concentration was estimated based on the $SiO_2/Al_2O_3$ ratio of zeolite (which is obtained from ICP-OES) and the fractions of Al(IV) and extraframework Al atoms for HUSY reported in literature[39-41] assuming that there were no counter-cations in the zeolite. This concentration was used for an estimation of the theoretical metal to acid sites ratios of the catalysts (Table 1), as the acidity of HUSY zeolites is affected neither by the low Pt contents nor by the applied thermal treatments[36]. Even though the best generic method to determine the concentration of Brønsted acid sites is pyridine temperature programmed desorption, the other methods work out effectively[41] for the catalysts examined in our work. The acid sites concentrations which were obtained by ammonia temperature programmed desorption, were used for the calculation of alternative values for the ratio of metal and acid sites. In addition, the Pt sites concentration was calculated with the Pt dispersion. In Supporting information Section S8, the procedure for estimation of the metal-acid sites ratio is reported.

The characteristics of the catalysts are reported in Table 1. Based on the results of $NH_3$-TPD, low Pt amounts do not impact the acid properties of Pt/HUSY catalysts[36]. Some larger particles were observed by TEM for 0.3 wt%Pt catalyst. Hence, the average particle size was slightly larger for that catalyst in comparison to the other catalysts. (Figure S4 in Supporting information)[23, 42].

**Table 1 Catalyst properties**

| **Catalyst Pt/HUSY*** | **0.07 wt% Pt** | **0.1 wt% Pt** | **0.3 wt% Pt** |
|---|---|---|---|
| Pt loading (wt%) [ICP] | 0.06 | 0.09 | 0.25 |
| Pt reduction degree (%) [$H_2$ TPR] | 65 | 48 | 36 |
| Pt dispersion (%) [$H_2$-$O_2$ titration] | 63 | 55 | 82 |
| Acidity (mmol/g) [$NH_3$ TPD] ** | 0.96 | 1.08 | 1.02 |
| Particle size (nm) | | | |
| [TEM] | 1.0 | 1.0 | 1.4 |
| [$H_2$-$O_2$ titration] | 1.6 | 1.2 | 1.3 |

| | | | |
|---|---|---|---|
| Specific surface area ($m^2/g$) [$N_2$ adsorption t-plot] | 500 | 514 | 570 |
| $n_{Pt}/n_{H+}$ x $10^3$ (mol/mol) | 1.1 | 1.6 | 7.1 |

* HUSY zeolite has $SiO_2/Al_2O_3$ ratio of 12.

** Acidity of pure HUSY zeolite with $SiO_2/Al_2O_3$ ratio of 12 (determined by $NH_3$-TPD) is 1.14 mmol/g.

### *2.3. Kinetic measurements*

Kinetic measurements were performed in a high-throughput kinetics setup (Zeton) which is dedicated for mechanistic investigations (HTK-MI)[43]. One block of the setup contains two parallel reactors with a length of 89 cm and an internal diameter of 11 mm, accommodated in a furnace that allows temperature control at three points in the reactor[43]. Hydrogen as reactant gas, and methane as an internal standard for analysis were used. Thermal mass flow controllers (Bronkhorst) regulate the gas inlet flow rates. The flowrate of liquid reactants is controlled by an HPLC pump (Knauer Azura P4.1s). A membrane back-pressure regulator (Equilibar) piloted with nitrogen controls the pressure in the system. The setup is completely heat-traced (to about 200°C) and the reactor effluent remains in the vapor phase. The reaction products were analyzed by gas chromatography (GC) (6850 Series II, Agilent Technologies) equipped with an FID and a non-polar capillary column (Agilent HP-PONA, 50 m x 200 µm x 0.5 µm polydimethylsiloxane). Representative gas samples of the reactor effluent were analyzed by GC x GC – FID/MS (Thermo Scientific TRACE, Interscience) consisting of two columns : a Rtx-1 PONA column (50 m x 250 µm x 0.25 µm) and a BPX 50 (2 m x 180 µm x 0.18 µm) as the second column. The first column is connected to the second column through a Sil tite. Both columns and a dual-state cryogenic modulator (liquid $CO_2$) are placed in the same oven. The analyses on the GC x GC setup were performed to determine the presence of particular products in the effluent[44, 45].

Reactants were *n*-octane (extra pure, 99+%), *n*-decane (99%) both purchased from Acros Organics, methylcyclohexane (ReagentPlus®,99%), purchased from Sigma Aldrich, and tert-butylcyclohexane (99+%), purchased from Fischer Scientific. Methane (N35, 99.95% purity) and hydrogen (N40, 99.99% purity) were supplied by AirLiquide.

The catalyst bed was prepared in such a manner to avoid mass and heat transfer limitations[46]. The catalysts were pelletized, crushed and sieved to a diameter between 100 and 200 µm and diluted with inert alumina particles (150 µm) (Final advanced materials) with a mass ratio of 1:3 (catalyst : inert particles). The summary of mass and heat transfer limitations verification for the performed experiments is shown in Section S9 Supporting information. The catalyst was reduced in the reactor at 723K with a hydrogen flow rate of 50 NL/h for 1 h. The temperature in the reactor was increased with a heating rate of 5 K/min.

The total flow rate of the liquid feed was set by the pump's control panel and verified by regularly measuring the weight of the reactant flask. A uniform composition of the reactant mixture was ensured by gentle stirring at specific time intervals. The peak areas ($A_i$) of the gas chromatograms were normalized (with Dietz calibration factors $CF_i$ [47]) to obtain the mass fraction $y_i$ of each component i ($ntot, resp$).

$$y_i = \frac{A_i CF_i}{\sum_{j=1}^{ntot,resp} A_j CF_j}$$

The obtained weight composition of the reactor effluent and the flow rate of the internal standard were used to determine the mass and molar flow rates. The mass balance is considered to be 'closed' if the total weight of products and unreacted reactant equals measured reactant mass flow rate within 5%. The mass balances, overall and per reactant in case of admixture experiments, were closed in all experiments. The mass flow rates of reactants and particular products are converted into molar flow rates $F^o_{feed,i}$ and $F_{feed,i}$, to calculate the total conversion of reactant i $X_i$.

$$X_i = \frac{F^o_{feed,i} - F_{feed,i}}{F^o_{feed,i}}$$

Selectivity towards all isomers (or different isomer groups) $S_{iso}$, and cracking products $S_{cr}$ are obtained by summation of all carbon molar flow rates of isomers/cracking products $S_i$ belonging to a particular group (with n products in the group) and division by the carbon products total flow rate. Corresponding yields of product i $Y_{i,j}$ are obtained by multiplication of selectivity and conversion of reactant j.

$$S_i = \frac{\sum_{i=1}^{n} F_i}{\sum_{j=1}^{nprod} F_j}$$

$$Y_{i,j} = S_i X_j$$

Space times $ST_i$ were calculated for every reactant in the mixture based on catalyst weight $W_{cat}$ and initial measured molar flow rate of the particular reactant $F^o_{feed,i}$.

$$ST_i = \frac{W_{cat}}{F^o_{feed,i}}$$

*2.4. Definition of the experimental space*

Model components for this experimental study were chosen so that the differences in their physico-chemical properties (see Introduction) ensure proper conclusions about the carbon number impact on the admixture effect. *n*-Octane and *n*-decane were selected as alkane model components, while methylcyclohexane and tert-butylcyclohexane were selected as cycloalkanes. These components are representative for oil fractions which are typically processed in hydroconversion units. The model components have a manageable, yet sufficiently extensive reaction network for observing the transition between ideal and non-ideal hydrocracking[12, 13]. In order to ensure the parallel comparison of the mixture and carbon number effects, and to avoid analytical complications due to a possible overlap of products, smaller model molecules were combined with larger ones of another hydrocarbon type (*n*-octane/tert-butylcyclohexane and *n*-decane/methylcyclohexane). Additionally, the working conditions of the experimental setup were taken into account, such that the reactor effluent always remains in the gas phase[43].

The general and physisorption properties of the model components (*n*-octane, *n*-decane, methylcyclohexane, and tert-butylcyclohexane) on different HUSY zeolites are presented in Supporting information – Section S10 (Table S6 – S7). Physisorption properties of cycloalkanes are assumed to be identical to those of an alkane with the same carbon number[25, 30, 32, 33, 48]. However, molecules with higher carbon numbers tend to exhibit a more pronounced physisorption[30, 32, 33, 48]. Henry coefficients of *n*-decane and tert-butylcyclohexane for HUSY zeolite with molar $SiO_2/Al_2O_3$ ratio of 12 are about an order of magnitude higher than those of *n*-octane and methylcyclohexane. Furthermore, the *n*-octane Henry

coefficient was about the double of that of methylcyclohexane. The reaction networks of the model components, obtained by the in-house developed program for reaction networks generation (RENGEP)[15], are compared in Table S8 (Supporting information Section S11). The composite activation energies of all acid catalyzed reaction families[10, 12, 13] which occur in alkane/cycloalkane hydroconversion are given in Table S9 (see Supporting information Section S11). The reaction networks of *n*-decane and tert-butylcyclohexane are far more extensive than the ones of *n*-octane and methylcyclohexane, the difference between the reaction network within cycloalkane model molecules being far more prominent than for alkanes. The reaction networks of *n*-octane and *n*-decane contain all acid catalyzed reaction families for alkanes. On the other hand, while impossible for methylcyclohexane, tert-butylcyclohexane can undergo exocyclic β-scissions. This fact, together with the carbon number impact, renders the tert-butylcyclohexane reaction network much more extensive than that of methylcyclohexane. The reaction network of tert-butylcyclohexane contains a large number of endocyclic β-scissions and reactions related to alkanes or the aliphatic part of cycloalkanes (Table S8). As ring-opening reactions have a very low rate, because of the significant entropy loss in the transition state formation[13] and consequent low pre-exponential factor[13], these reactions are not expected to occur to a significant extent. To verify this, the effluent of pure tert-butylcyclohexane hydroconversion was analyzed by GC x GC - MS. These qualitative analyses show a negligible amount of formed alkanes - in Figure 4 is indicated the only significant peak belonging to ring-opening products (dibranched decane isomer) (see Supporting information Section S12). Based on mass balances, no secondary cracking of ring-opening product was found in all performed experiments.

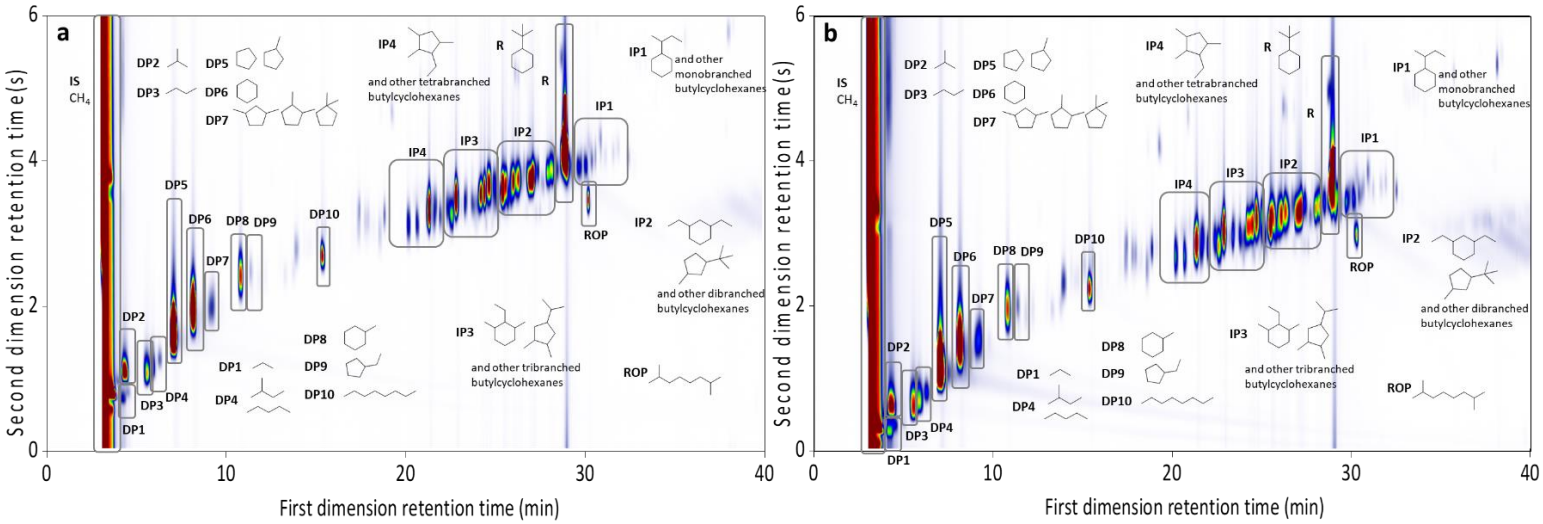


276 **Figure 4 GC x GC chromatograms of tert-butylcyclohexane hydroconversion over 0.07 wt%Pt/HUSY at 10 bar, about 600 kg**

277 **s/mol and (a) 523 K (conversion of 65%) and (b) 543 K (conversion of 77%)**

278 The operating conditions were selected to allow appropriate comparison of the kinetic behavior of the
279 different model components in mixtures. The partial pressure of all model components was kept constant
280 at 0.05 bar. In order to fulfill this condition, the hydrogen-to-hydrocarbon molar ratio ($H_2$/HC) had to be
281 adjusted when total pressure or feed composition were changed. The hydrocarbon partial pressure of 0.05
282 bar was selected to obtain a gaseous reactor effluent. While a low $H_2$/HC ratio can have an impact on the
283 reaction performances[24], it is expected that the impact is negligible at the selected high $H_2$/HC ratio.
284 Experiments were performed at two different total pressures, so that ideal hydrocracking occurrence can
285 be simply diagnosed[24].

286 The 0.1 wt%Pt catalyst, i.e., the one with the middle loading of Pt, exhibited ideal hydrocracking for pure
287 *n*-octane and methylcyclohexane, while the 0.07wt%Pt did not[16]. These results for pure *n*-octane and pure
288 methylcyclohexane (over both catalysts) were used for comparison in this research as well. Other feeds
289 were studied over 0.3 wt%Pt and 0.07 wt%Pt catalysts. As *n*-decane is more reactive than n-octane and
290 requires higher ratio of metal to acid sites for ideal hydrocracking, the catalyst with three times higher Pt
291 loading (0.3 wt%Pt) was used in the experiments. Temperature and flow rates were set such that a wide
292 range of conversions for all pure reactants is ensured (10-90% for *n*-octane, 40-90% for *n*-decane, 10-45%

for methylcyclohexane, and 40-90% for tert-butylcyclohexane). In that way, kinetic performances can be adequately compared. The feed with an equimolar mixture of reactants is expected to exhibit the most representative admixture effect. As the goal is to study the impact of the carbon number, experiments with the equimolar feed of *n*-decane and tert-butylcyclohexane were not performed. as it is expected to lead to the same conclusions as the experiments with the feed of *n*-octane and methylcyclohexane[16]. Moreover, the analysis of experimental data could become more challenging as decane isomers are ring-opening products of tert-butylcyclohexane. Table 2 summarizes the reaction conditions.

**Table 2 Reaction conditions for investigated model components over : (1) well-balanced catalyst - 0.1 wt%Pt/HUSY (for pure *n*-octane and pure methylcyclohexane) and 0.3 wt%Pt/HUSY (for other feeds) and (2) poorly-balanced catalyst – 0.07 wt%Pt/HUSY**

| Catalyst | Feed (mol/mol) | Space time (kg s/mol) | Temperature (K) | Pressure (bar) | $H_2$ / HC (mol/mol) | Partial pressure of reactants (bar) |
|---|---|---|---|---|---|---|
| (1) | *n*-octane / tert-butylcyclohexane | | | | | |
| | 1 : 0 * | 200 - 1200 | 523 ; 543 | 10 ; 20 | 200 ; 400 | 0.05 |
| | 0 : 1 | 250 - 1400 | 523 ; 543 | 10 ; 20 | 200 ; 400 | 0.05 |
| | 1 : 1 | 250 - 1400 | 523 ; 543 | 10 ; 20 | 100 ; 200 | 0.05 ; 0.05 |
| | *n*-decane / methylcyclohexane | | | | | |
| | 1 : 0 | 40 - 250 | 523 ; 543 | 10 ; 20 | 200 ; 400 | 0.05 |
| | 0 : 1 * | 200 - 1400 | 523 ; 543 | 10 ; 20 | 200 ; 400 | 0.05 |
| | 1 : 1 | 40 - 250 | 523 ; 543 | 10 ; 20 | 100 ; 200 | 0.05 ; 0.05 |
| (2) | *n*-octane / tert-butylcyclohexane | | | | | |
| | 1 : 0 * | 200 - 1200 | 523 ; 543 | 10 ; 20 | 200 ; 400 | 0.05 |
| | 0 : 1 | 250 - 1400 | 523 ; 543 | 10 ; 20 | 200 ; 400 | 0.05 |
| | 1 : 1 | 250 - 1400 | 523 ; 543 | 10 ; 20 | 100 ; 200 | 0.05 ; 0.05 |
| | *n*-decane / methylcyclohexane | | | | | |
| | 1 : 0 | 200 - 1400 | 523 ; 543 | 10 ; 20 | 200 ; 400 | 0.05 |
| | 0 : 1 * | 200 - 1400 | 523 ; 543 | 10 ; 20 | 200 ; 400 | 0.05 |
| | 1 : 1 | 200 - 1400 | 523 ; 543 | 10 ; 20 | 100 ; 200 | 0.05 ; 0.05 |

* These experiments were performed within the study on the interplay between metal-acid balance and cycloalkane admixture effect on *n*-octane hydroconversion[16].

## 3. Results and discussion

The role of the molecule carbon number has been examined by kinetic measurements with mixtures of alkanes and cycloalkanes with significantly different physico-chemical properties, i.e., *n*-octane/tert-butylcyclohexane and *n*-decane/methylcyclohexane. As the metal-to-acid sites ratio represents a key parameter to control the course of hydrocracking reaction, catalysts have been selected which, on the one hand, ensure ideal hydrocracking for pure model (cyclo)alkanes, and on the other hand, which do not (see Section 2.4 for details).

### *3.1. n-Octane and tert-butylcyclohexane hydroconversion*

In our previous work, it was found that methylcyclohexane admixture does not impact *n*-octane conversion over 0.1 wt%Pt/HUSY catalyst[16]. As a higher total pressure results in a decrease of *n*-octane conversion, ideal hydrocracking of pure *n*-octane occurs over this catalyst, which is further referred to as 'well-balanced'. On the other hand, by lowering the metal content of the catalyst (to 0.07 wt%Pt), the *n*-octane conversion decreased and became independent of the total pressure. This is indicative of nonideal hydrocracking over this catalyst, which is further referred to as 'poorly-balanced'. In contrast to the well-balanced catalyst, methylcyclohexane admixture has slightly decreased *n*-octane conversion over the poorly-balanced catalyst. This impact was more prominent with an even lower Pt loading[16].

#### *3.1.1. Experimental results*

The *n*-octane conversion when fed pure, and in 1:1 n/n mixtures with methylcyclohexane[16], and tert-butylcyclohexane, is compared in Figure 5 over the well-balanced and poorly-balanced catalyst, at a total pressure of 10 bar (the experimental results at 20 bar and the comparison at both pressures are shown in Supporting information Figure S9 and Figure S10). For the well-balanced catalyst the *n*-octane conversion does not change in the presence of methylcyclohexane[16], whereas it does significantly decrease, i.e., to

25% of its original value, upon tert-butylcyclohexane admixture. No impact of total pressure on *n*-octane conversion was observed over the narrow range of conversions (up to 25%) obtained upon admixture of tert-butylcyclohexane (see Figure S10 and S11 in Supporting information), suggesting that the admixture of a heavier cycloalkane could shift the reaction regime for *n*-octane from ideal to nonideal.

Figure 5b shows the impact of cycloalkane admixture on the *n*-octane conversion over the poorly-balanced catalyst. While methylcyclohexane admixture in this impacts the *n*-octane conversion, albeit only slightly, the latter decreases significantly upon tert-butylcyclohexane admixtures. Surprisingly, the *n*-octane conversion range over both well- and poorly-balanced catalyst was similar. In summary, with the increase of the cycloalkane size, its negative impact on *n*-alkane hydrocracking becomes more important.

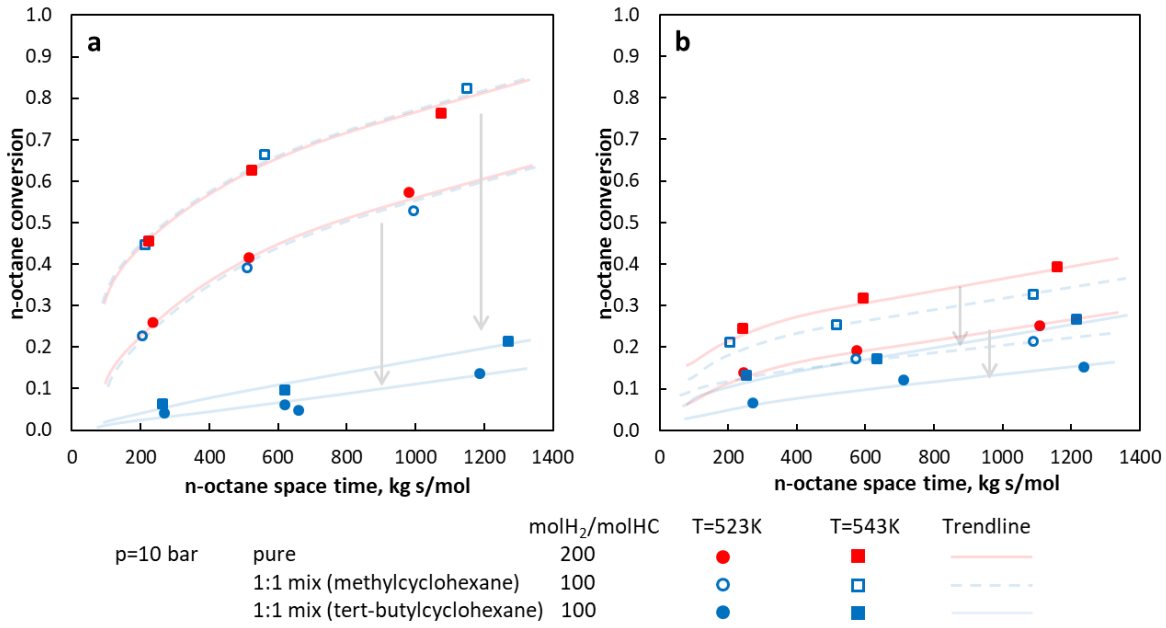


**Figure 5 *n*-Octane conversion when fed pure and in 1:1 n/n mixture with methylcyclohexane and tert-butylcyclohexane, at 523 K and 543 K and 10 bar as a function of space time calculated based on *n*-octane flow rate over (a) 0.3wt%Pt/HUSY (well-balanced), and (b) 0.07wt%Pt/HUSY (poorly-balanced catalyst)**

To gain more insight in the cycloalkane admixture impact, and particularly of tert-butylcyclohexane, on the hydrocracking mechanism, the *n*-octane isomer yields are compared in Figure 6. It had been already observed before that methylcyclohexane admixture did not change the *n*-octane isomer yield[16]. The

constant *n*-octane conversion and isomer yield showed that methylcyclohexane has no prominent tendency to shift the hydrocracking regime from ideal to nonideal[16]. On the other hand, it can be noticed, already at low conversions, that the *n*-octane isomer yield is lower with tert-butylcyclohexane as co-reactant, see Figure 6a (magnified Figure 6 is given as Figure S12 in Supporting information). For the poorly-balanced catalyst, the *n*-octane isomer yield with tert-butylcyclohexane admixture becomes even lower (Figure 6b). The combined effects of tert-butylcyclohexane admixture and a poorly-balanced catalyst, have resulted in a significant extent of *n*-octane cracking products already at low conversions. In comparison to methylcyclohexane, tert-butylcyclohexane has a much higher tendency to cause the transition from ideal to nonideal hydrocracking of *n*-octane. No specific impact of operating conditions (pressure and temperature) on the *n*-octane isomer yield with tert-butylcyclohexane admixture could be identified over both well- and poorly-balanced catalyst. This is believed to originate from the low *n*-octane conversions which results from the significant inhibition by tert-butylcyclohexane.

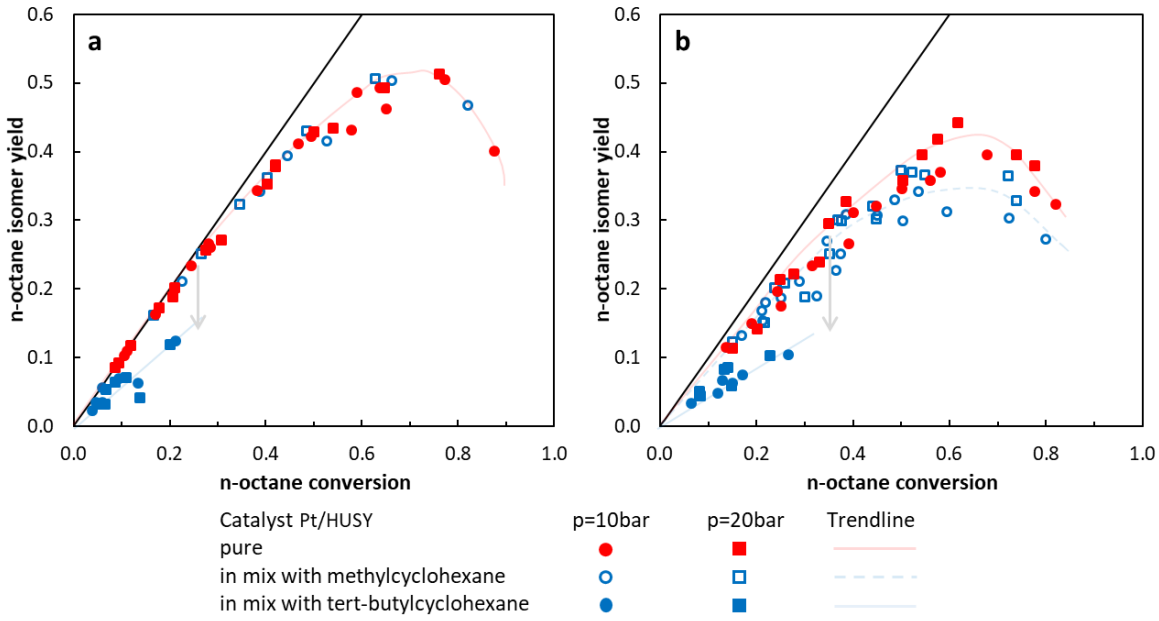


**Figure 6 *n*-Octane isomer yields as a function of *n*-octane conversion, when fed pure and in 1:1 n/n mixture with methylcyclohexane and with tert-butylcyclohexane, at conditions of Figure 5 and Figure S9 over (a) 0.3wt%Pt/HUSY (well-balanced), and (b) 0.07wt%Pt/HUSY (poorly-balanced)**

In order to understand the impact of tert-butylcyclohexane on *n*-octane hydrocracking, it is necessary to understand the hydrocracking kinetic behavior of pure tert-butylcyclohexane. For pure tert-butylcylohexane and an equimolar mixture with *n*-octane, the same reaction conditions were set, keeping the partial pressure of reactants constant (Table 2). The tert-butylcyclohexane conversion at a total pressure of 10 bar is shown in Figure 7. The experimental results at 20 bars and the comparison of all results are given in Supporting information Figure S13 and Figure S14, respectively. An increase in total pressure did not change the pure tert-butylcyclohexane conversion over both catalysts. This indicates that the metal function was not sufficiently strong to ensure quasi-equilibrated (de)hydrogenation of tert-butylcyclohexane and its products. Therefore, even the catalyst with the highest Pt loading behaves as a poorly-balanced one for tert-butylcyclohexane hydrocracking. Tert-butylcyclohexane conversions are higher than for *n*-octane, indicating high reactivity. The tert-butylcyclohexane conversion only being slightly lower with lower Pt loading (0.07 wt%Pt) confirms the high reactivity of tert-butylcyclohexane at the examined reaction conditions. This high reactivity can be attributed to the extensive acid catalyzed reaction network and the presence of tertiary carbon atoms in the reactant[13].

Concerning the potential *n*-octane admixture impact on the cycloalkane, no such impact was found on tert-butylcyclohexane conversion over any of the investigated catalysts – the conversion only depended on the partial pressure, temperature, and space time of the cycloalkane. This is in line with the observation from our previous work, where *n*-octane admixture did not impact the conversion of methylcyclohexane[16], indicating a predominant role of cycloalkane in alkane/cycloalkane hydroconversion.

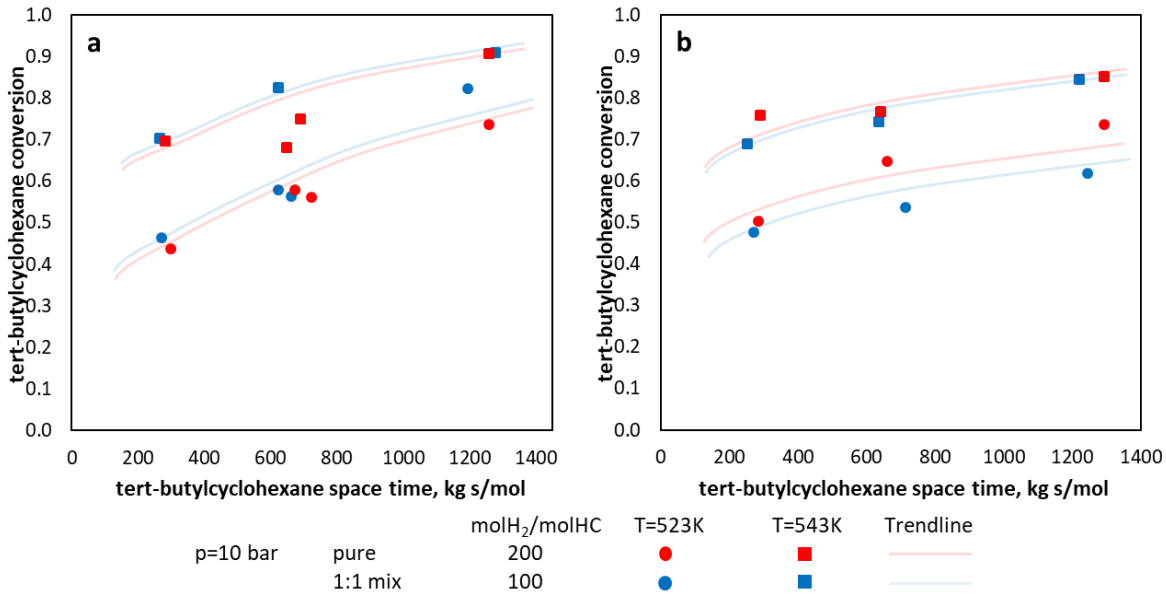


**Figure 7 tert-Butylcyclohexane conversion when fed pure and in 1:1 n/n mixture with *n*-octane, at 523 K and 543 K and 10 bar as a function of space time calculated based on tert-butylcyclohexane flow rate over (a) 0.3wt%Pt/HUSY, and (b) 0.07wt%Pt/HUSY**

Figure 8 depicts the evolution of the cyclic isomers yield with tert-butylcyclohexane conversion over both catalysts. The butylcyclohexane cyclic isomer yield for the well-balanced catalyst does not follow a unique curve as a function of conversion, see Figure 8a. At higher temperatures the cyclic isomer yield is lower. Additionally, there is a more prominent impact of total pressure: with higher total pressure, the cyclic isomer yield significantly increases over the whole conversion range, regardless of the temperature.

For alkanes, in the case of nonideal hydrocracking, higher temperature also lead to lower isomer yields, while an increasing total pressure induces a higher isomer yield[24]. The activation energies of, or at least the most kinetically relevant reaction families included in cycloalkane hydrocracking are similar and comparable with the corresponding ones in alkane hydrocracking[13] (see Supporting information Table S9). Therefore, similar trends of cyclic isomer yields with a change of operating conditions can be expected when the concentration of metal sites is not sufficient to ensure quasi-equilibrated dehydrogenation.The experimental findings herein for cyclic isomers in tert-butylcyclohexane hydroconversion are in line with

this[24]. Additionally, the impact of *n*-octane admixture on the butylcyclohexane isomer yield over the well-balanced catalyst also depends on the operating conditions.

The use of a poorly-balanced catalyst further (Figure 8b) decreases the cyclic isomers yields, which tend to become almost pressure and temperature independent. No impact of *n*-octane admixture on the cyclic isomer yield is observed for this. This overall behavior is attributed to the low isomer yields over this (for tert-butylcyclohexane, extremely) poorly-balanced catalyst, rather than any kinetic phenomenon: the low yields to cyclic isomers (20-30%) make that any impact of experimental conditions is of the same order of magnitude of the experimental error (up to 5%).

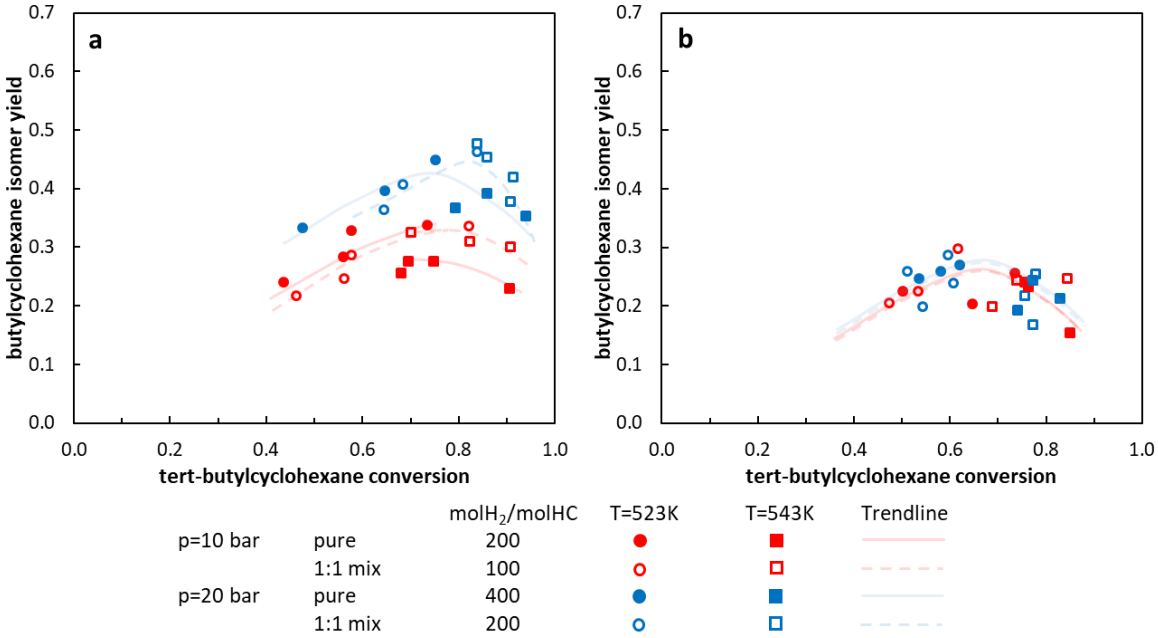


**Figure 8 Butylcyclohexane isomer yields as a function of tert-butylcyclohexane conversion, when fed pure and in 1:1 n/n mixture with *n*-octane, at conditions of Figure 7 and Figure S13 over (a) 0.3wt%Pt/HUSY, and (b) 0.07wt%Pt/HUSY**

### *3.1.2. Experimental findings summary*

The extensive experimental study with *n*-octane and tert-butylcyclohexane as model components, supported by the experimental findings from our previous work[16], resulted in the following key findings for the comparison of the admixture impact of methylcyclohexane and tert-butylcyclohexane on *n*-octane:

(a1) the *n*-octane conversion was significantly decreased by tert-butylcyclohexane over both well- and poorly-balanced catalysts for *n*-octane (Figure 5a and 5b);

(a2) tert-butylcyclohexane admixture decreased significantly the *n*-octane isomers yield over both well- and poorly-balanced catalysts (Figure 6a and 6b);

(a3) tert-butylcyclohexane had a more pronounced impact on the *n*-octane isomers yield than methylcyclohexane (Figure 6a and 6b);

(a4) even the catalyst with higher metal content (0.3 wt%Pt), which is well-balanced for *n*-decane, proved to be poorly-balanced for tert-butylcyclohexane hydroconversion (Figure 7a, 7b, 8a, and 8b);

(a5) the tert-butylcyclohexane conversion was not impacted by *n*-octane admixture over both studied catalysts (Figure 7a and 7b); and

(a6) in general, *n*-octane admixture did not impact the yield of tert-butylcyclohexane cyclic isomers (Figure 8a and 8b).

*3.1.3. Discussion*

To evaluate and understand the impact of the cycloalkane size (mixture with *n*-octane), it is necessary to analyze the properties of the feed molecules. The different carbon number of methylcyclohexane versus tert-butylcyclohexane creates a significant contrast in their physico-chemical properties (see also Section 2.4). The reaction network of tert-butylcyclohexane is far more extensive than the one of methylcyclohexane, but also than that of *n*-octane (Table S8). Contrary to the reaction network of methylcyclohexane, which is limited to a couple of rearrangements within the hydrocarbon ring yielding only four cyclic isomers[13], tert-butylcyclohexane undergoes dealkylation (exocyclic β-scissions) and ring-opening reactions (endocyclic β-scissions), but also rearrangement reactions of the aliphatic branch (PCP branching). As already discussed before (see Section 2.4), only negligible amount of ring-opening products were observed (Figure 4). A somewhat more negative standard protonation enthalpy can be expected for tert-butylcyclohexane because of its higher carbon number[10] and cyclic structure[49], both contributing to

433 the stability of the generated carbenium ions. Therefore, a stronger protonation is expected for tert-
434 butylcyclohexane compared to methylcyclohexane.
435 Methylcyclohexane was inferred to adsorb on metal sites more preferentially than *n*-octane[16]. Hence,
436 (de)hydrogenation reactions of methylcyclohexane occur more readily. Due to a lack of the studies of
437 cycloalkane adsorption onto metals, the carbon number impact on the metal catalyzed phenomena has to
438 be deduced from our kinetic observations. The working hypothesis is that tert-butylcyclohexane adsorbs,
439 in general, more strongly and undergoes (de)hydrogenation reactions faster than methylcyclohexane,
440 owing to the higher adsorption stability of longer carbon chains and a larger number of possible
441 (de)hydrogenation reactions.
442 Cycloalkanes physisorb on a zeolite-based catalyst with a similar strength as alkanes with the same carbon
443 number[13, 25, 29] Hence, cycloalkanes with higher carbon number will be preferably physisorbed in the zeolite
444 pores[10, 30-33, 48, 50]. Consequently, based on Henry coefficients over the zeolite, tert-butylcyclohexane
445 physisorbs ten times stronger than both *n*-octane and methylcyclohexane.
446 Experimental findings (a1) and (a2) are strong evidence of tert-butylcyclohexane admixture impact. Ideal
447 hydrocracking of *n*-octane could not be ensured in the mixture, indicating that the available metal to acid
448 sites ratio for *n*-octane conversion was reduced by tert-butylcyclohexane. The catalyst with 0.1 wt%Pt
449 loading was previously found to be well-balanced for pure *n*-octane hydrocracking[16]. In the present work,
450 due to, among other reasons, the expected more significant impact of tert-butylcyclohexane compared to
451 methylcyclohexane, more platinum was impregnated (0.3 wt%Pt) to achieve even better well-balanced
452 catalyst. Nevertheless, the admixture of tert-butylcyclohexane had a negative impact even over this
453 catalyst with the enhanced metal to acid sites ratio.
454 As already discussed, compared to *n*-octane, tert-butylcyclohexane was expected to be more favorably
455 adsorbed onto the metal sites[16], protonated[10, 49], and physisorbed[10, 30-33, 48, 50]. Competitive physisorption
456 impacts only the concentration of physisorbed molecules and, consequently, as it occurs prior to

457 adsorption onto metal sites, does not affect the available metal to acid sites ratio in a negative way. In that
458 sense, the preferential physisorption of tert-butylcyclohexane compared to *n*-octane (by an order of
459 magnitude), can even slightly improve the available metal to acid sites ratio for *n*-octane, because a lower
460 physisorbed concentration of *n*-octane will require fewer metal active sites for equilibrated
461 (de)hydrogenation. The kinetic impact of tert-butylcyclohexane, is, hence, potentially explained by
462 preferred adsorption onto metal sites (followed by (de)hydrogenation reactions) and/or preferred
463 protonation onto acid sites. If these two effects were of comparable intensity, the *n*-octane hydrocracking
464 rate would decrease, but the available metal to acid sites ratio for *n*-octane would remain similar. As a
465 consequence, there would be no significant change on the selectivity to *n*-octane isomers. The observed
466 reduction of conversion (a1) and isomer selectivity (a2) over both catalysts point towards a lower effective
467 metal to acid ratio. More precisely, the major impact of tert-butylcyclohexane is on the metal sites. The
468 preferential adsorption on metal sites and the numerous dehydrogenation reactions of tert-
469 butylcyclohexane indicate that a high concentration of metal sites is needed for tert-butylcyclohexane
470 ideal hydrocracking. Due to this phenomenon, as observed experimentally (a3), the admixture effect on
471 isomer yield became far more obvious with tert-butylcyclohexane than with methylcyclohexane.
472 Tert-butylcyclohexane exhibited very high reactivity, irrespective of the Pt loading. All catalysts used were
473 found to be poorly-balanced for tert-butylcyclohexane, not being able to establish ideal hydrocracking for
474 this component (experimental finding (a4)). Based on experimental findings (a5) and (a6), the tert-
475 butylcyclohexane hydrocracking can be considered very resistant to an impact of *n*-octane admixture. This
476 was evident even for methylcyclohexane[16] and, hence, it is logic that the same occurs with tert-
477 butylcyclohexane.
478 The nature of the admixture effect is not changed with cycloalkane components with higher carbon
479 numbers – it is mainly related to the preferential adsorption to metal sites and the extent of the
480 (de)hydrogenation reaction network. The effect does become more pronounced with the carbon number

481 of the cycloalkane. Apparently, *n*-octane does not impact any of the cycloalkane hydrocracking steps over
482 bifunctional catalysts.

483 *3.2. n-Decane and methylcyclohexane hydroconversion*

484 To complete the experimental analysis of the role of carbon number on the admixture effect, kinetic tests
485 with an *n*-alkane with different physico-chemical properties than *n*-octane were performed. *n*-Decane was
486 selected as a new model component due to its stronger adsorption affinities and more extensive acid
487 catalyzed reaction network. Evidently, the kinetics investigation was performed at ideal as well as at
488 nonideal hydrocracking conditions.

489 *3.2.1.Experimental results*

490 Figure 9 depicts the *n*-decane conversion when it is fed pure and in a 1:1 n/n mixture with
491 methylcyclohexane over the well-balanced (Figure 9a) and the poorly-balanced (Figure 9b) catalyst at a
492 total pressure of 10 bar. (The experimental results at a total pressure of 20 bar and comparison of all
493 results are given in Supporting information, Figure S15 and S16, respectively.) Note that Figure 9a shows
494 *n*-decane conversion at lower space times compared to Figure 9b. *n*-Octane conversion when it is fed pure
495 and in a 1:1 n/n mixture with methylcyclohexane over well-balanced and over poorly-balanced catalyst at
496 a total pressure of 10 bar is shown on Figure 5a and 5b, respectively. The pure *n*-decane conversion
497 decreased at higher total pressures. Although the differences in conversion are relatively low (5-10%), they
498 occur at both temperatures and along the investigated space time range. When the (de)hydrogenation
499 reactions are quasi-equilibrated, i.e., when ideal hydrocracking occurs, the distribution between saturated
500 and unsaturated products will lean more towards the saturated ones upon a total pressure increase due
501 to thermodynamic reasons (Le Chatelier's principle)[24]. Consequently, the supply of alkene intermediates
502 to acid active sites is lowered, as well as the concentration of alkyl-carbenium ions, and, finally, the
503 conversion[4, 7]. Increased hydrogen partial pressures favor hydrogenation of produced alkene
504 intermediates and, hence, decreases the chance of re-protonation and consecutive acid catalyzed

reaction. The kinetic behavior of *n*-decane over the well-balanced catalyst proves that the metal function was strong enough to ensure the equilibration of the dehydrogenation reactions. Ideal hydrocracking of *n*-decane occurred over this catalyst at the employed experimental conditions.

Figure 9b shows the *n*-decane conversion over the poorly-balanced catalyst. The total pressure change, while keeping the partial pressure of *n*-decane constant, did not impact the conversion. This observation confirms, as expected that nonideal hydrocracking of *n*-decane occurs over this catalyst, as it was already exhibiting non-ideal hydrocracking behavior for *n*-octane see Figure 5b[16].

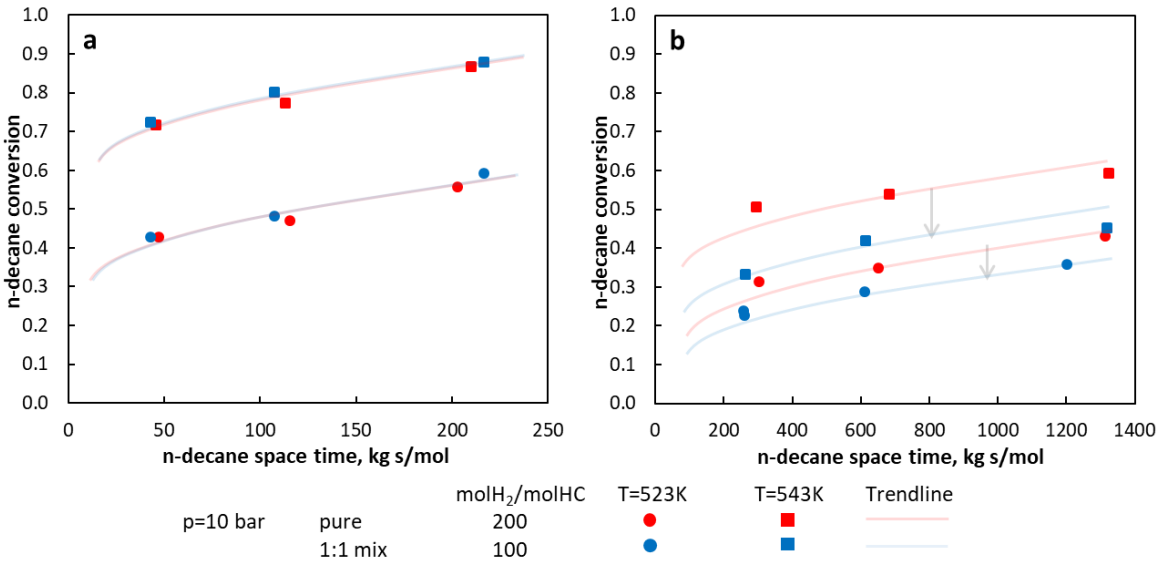


**Figure 9 *n*-Decane conversion when fed pure and in 1:1 n/n mixture with methylcyclohexane, at 523 K and 543 K and 10 bar as a function of space time calculated based on *n*-decane flow rate over: (a) 0.3wt%Pt/HUSY (well-balanced), and (b) 0.07wt%Pt/HUSY (poorly-balanced)**

The addition of methylcyclohexane did not change the *n*-decane conversion over the well-balanced catalyst (Figure 9a) like in the case of *n*-octane (Figure 9b). On the other hand, the *n*-decane conversion over the poorly-balanced catalyst was significantly decreased by methylcyclohexane admixture, see Figure 9b. Furthermore, the impact on *n*-decane was much more significant compared to *n*-octane (Figure 9b and Figure 5b). The more extended *n*-decane acid catalyzed reaction network is deemed responsible for this. Methylcyclohexane, despite being a smaller molecule than *n*-decane and, hence, being less preferentially

physisorbed in the zeolite pores, does impact *n*-decane hydroconversion. The lower *n*-decane conversion in admixture with methylcyclohexane over 0.07 wt%Pt catalyst is a result of a lower effective metal to acid sites ratio for *n*-decane, which is, in the end, the consequence of the preferential adsorption of cycloalkanes on the metal sites[16].

The isomer yield curve obtained on the well-balanced catalyst does not depend on the operating conditions and reaches a maximum of about 60% at 80% conversion (Figure 10). This confirms the ideal hydrocracking of *n*-decane over this catalyst. In addition, methylcyclohexane admixture did not impact the isomer yield. By lowering the Pt content, the *n*-decane isomer yield significantly decreased (from 60% to 20%), see Figure 10. The impact of pressure on isomer yield of pure *n*-decane over the poorly-balanced catalyst is also noticeable - the isomer yield at 20 bar is about 20%, comparing to a yield of about 13% at 10 bar pressure. This is as expected for nonideal hydrocracking of *n*-decane[24]. Regarding the mixture effect, the *n*-decane isomer yield was not notably changed by methylcyclohexane admixture over the poorly-balanced catalyst.

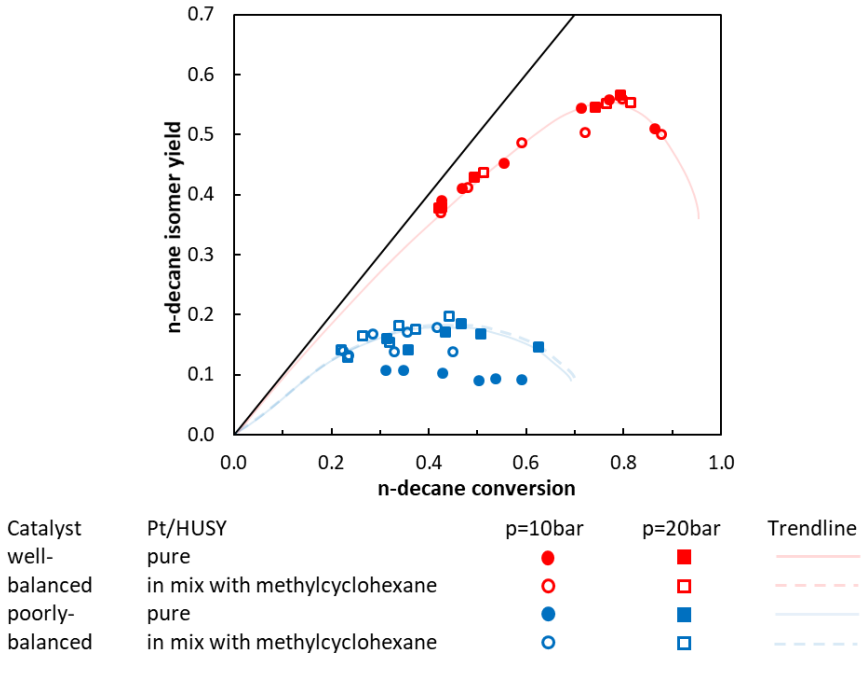

**Figure 10 *n*-Decane isomer yields as a function of *n*-decane conversion, when fed pure and in 1:1 n/n mixture with methylcyclohexane, at conditions of Figure 9 (a and b) and Figure S15 (a and b) over well-balanced (0.3wt%Pt/HUSY), and poorly-balanced (0.07wt%Pt/HUSY) catalyst**

Figure 11 shows the conversion of pure methylcyclohexane and in equimolar mixture with *n*-decane over the well-balanced (Figure 11a) and the poorly-balanced (Figure 11b) catalyst, at a total pressure of 10 bar, as a function of space time. The conversion at 20 bar and comparison of all results are given in Supporting information Figure S17 and S18, respectively. In contrast to what happened with *n*-octane, the methylcyclohexane conversion was decreased by *n*-decane admixture over both catalysts. At the same time, methylcyclohexane conversion exhibited an identical trend with the pressure change as in the case when methylcyclohexane is fed pure to the reactor (Figure 11a and Figure S18a), indicating that ideal hydrocracking occurs in both cases. Such behavior can be explained by the significantly stronger physisorption affinity of *n*-decane compared to methylcyclohexane (i.e., more than ten times), which results in a lower physisorbed methylcyclohexane concentration. The methylcyclohexane conversion also decreased over the poorly-balanced catalyst (Figure 11b). Despite the relatively low conversion for pure methylcyclohexane, the conversion further decreased as a result of *n*-decane admixture. In contrast to *n*-octane[16], *n*-decane admixture led to a negative impact on methylcyclohexane conversion regardless of the catalyst.

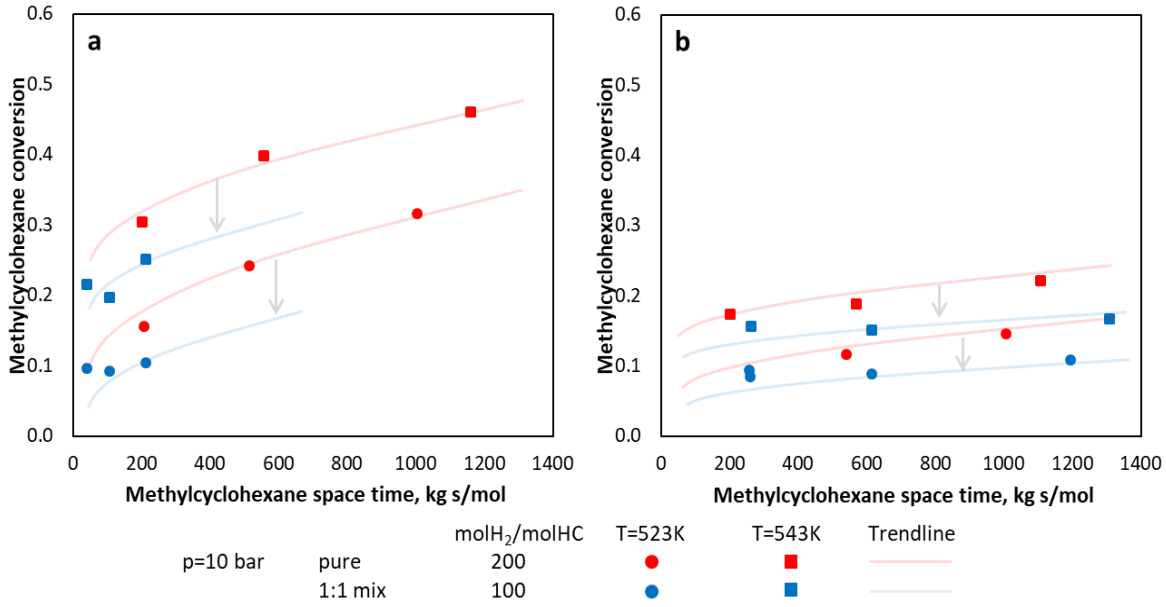


**Figure 11 Methylcyclohexane conversion when fed pure and in 1:1 n/n mixture with *n*-decane, at 523 K and 543 K and 10 bar as a function of space time calculated based on methylcyclohexane flow rate over (a) 0.3wt%Pt/HUSY, and (b) 0.07wt%Pt/HUSY**

### *3.2.2. Experimental findings summary*

The thorough experimental campaign with *n*-decane and methylcyclohexane as model components resulted in the following key experimental findings concerning the parallel analysis of *n*-octane and *n*-decane as model molecules in mixture with methylcyclohexane:

(b1) the *n*-decane conversion and isomer yield were not affected by methylcyclohexane over a well-balanced catalyst (Figure 9a);

(b2) over a poorly-balanced catalyst, methylcyclohexane admixture decreased the *n*-decane conversion (Figure 9b);

(b3) the impact of methylcyclohexane was more prominent on *n*-decane than on *n*-octane conversion (Figure 9);

(b4) *n*-decane admixture decreased the methylcyclohexane conversion, over both well- and poorly-balanced catalyst (Figure 11a and 11b); and

(b5) the *n*-decane impact on methylcyclohexane hydroconversion was significantly more pronounced than the impact of *n*-octane (Figure 5 and Figure 11).

### *3.2.3.Discussion*

The role of the *n*-alkane molecule size (in admixture with methylcyclohexane) can be determined by a comparison of the experimental investigations reported above with *n*-octane and *n*-decane. Regarding the reaction network, *n*-decane has a more extensive reaction network than *n*-octane. In contrast to tert-butylcyclohexane versus methylcyclohexane, no new reaction families appear in the reaction network of *n*-decane compared to *n*-octane[12]. As a consequence of the higher number of acid-catalyzed elementary steps[23], a higher reactivity of *n*-decane in comparison to *n*-octane is expected and has been indeed reported[12, 24]. On the other hand, the protonation enthalpies of *n*-octane and *n*-decane are slightly different[10]. As already mentioned before (Section 3.1), the physisorption affinity of hydrocarbons on zeolites increases with its carbon number[6-9, 12, 13]. Whether there is a carbon number dependence of *n*-alkane adsorption to metal sites, cannot be assumed based on physisorption affinity.

The well-balanced catalyst for *n*-decane hydrocracking remained exhibiting ideal hydrocracking behavior upon methylcyclohexane admixture with *n*-decane (experimental finding (b1)). Over the poorly-balanced catalyst, methylcyclohexane lowered the *n*-decane conversion (experimental finding (b2) and (b3)). This impact seems to be more prominent for *n*-decane than for *n*-octane (experimental finding (b5)). At the same time, methylcyclohexane did not impact the *n*-decane isomer yield (which was already very low for pure *n*-decane). The poorly-balanced catalyst is further from ideal hydrocracking for *n*-decane than for *n*-octane because of the higher reactivity of *n*-decane. Hence, the overall methylcyclohexane impact on *n*-decane conversion in this case could represent a combination of two parameters – metal to acid sites ratio and methylcyclohexane effect. As methylcyclohexane admixture does not impact the isomer yield of *n*-decane over the poorly-balanced catalyst, it seems that the impact of the metal to acid sites ratio prevails over the admixture impact. Nevertheless, the fact that methylcyclohexane inhibits *n*-decane

hydrocracking, indicates that its adsorption onto metal sites is stronger than the adsorption of *n*-decane, a significantly larger (*n*-alkane) molecule.

Based on experimental finding (b4), in contrast to *n*-octane, there is an impact of *n*-decane admixture on methylcyclohexane conversion. The catalyst with 0.3 wt%Pt was well-balanced for both pure *n*-decane and pure methylcyclohexane, but in admixture with *n*-decane, the methylcyclohexane conversion decreased. Such behavior points towards an admixture impact on metal or acid active sites. Lower conversion in this case can only be the result of a lower methylcyclohexane concentration in catalyst pores. *n*-Decane physisorbs 10 times stronger than methylcyclohexane, resulting in a lower concentration of methylcyclohexane in the zeolite pores. This is validated by the more pronounced impact of *n*-decane than that of *n*-octane on methylcyclohexane hydrocracking (experimental finding (b5)).

*n*-Decane and tert-butylcyclohexane have been experimentally found as more reactive compounds compared to *n*-octane and methylcyclohexane. *n*-Decane conversion was more than two times higher than *n*-octane at similar operating conditions over the well- and poorly-balanced catalysts. At the same time, tert-butylcyclohexane was almost four times more reactive than methylcyclohexane over the investigated catalysts. Although both molecules have the same carbon number and a comparable number of acid catalyzed reactions, kinetic tests have evidenced a much higher reactivity of tert-butylcyclohexane. This high reactivity is very likely caused by the increased individual rate and total number of dehydrogenation reactions of the cycloalkane. So, the apparent mixture effect can be even presumed by observing hydroconversion of pure components. Nevertheless, the observation of significantly higher reactivity of cycloalkanes as opposed to alkanes was not possible by comparison of the *n*-octane and methylcyclohexane conversion. The latter component had a quite low reactivity in comparison to both *n*-octane and tert-butylcyclohexane, due to the limited reaction network that included only isomerization to four different isomers[13, 16].

Another aspect that needs to be considered is the ratio of metal to acid sites. The admixture impacts became more obvious when metal site concentration is around the limit which ensures equilibrated dehydrogenation. Though it is challenging to experimentally observe this unique metal-to-acid sites ratio, taking into account the impacts observed in non-ideal regime, adequate conclusions can be reached for the transition between regimes.

In short, the alkane admixture effect is related to the hydrocarbon physisorption within the zeolite pore system. This effect becomes more pronounced with the difference in carbon numbers of the components involved, but it is still less prominent than cycloalkane impact on adsorption to metal site. No specific impact of *n*-alkane admixture with cycloalkanes was observed that could be related to metal and acid sites and their kinetics. On the other hand, cycloalkanes impact *n*-alkane hydroconversion over the bifunctional catalyst with a very limited influence on the difference in carbon number.

## *4. Conclusions*

The impact of carbon number on the mixture effects in the hydroconversion of alkanes and cycloalkanes was explored by kinetic experiments over well- and poorly-balanced Pt/HUSY catalysts.

*n*-Octane conversion and isomer yield are lowered as a consequence of cycloalkane admixture. This effect, which was already observed upon methylcyclohexane admixture to *n*-octane, only became more pronounced upon tert-butylcyclohexane admixture over both well- and poorly-balanced catalysts. Despite its lower carbon number, methylcyclohexane was able to negatively impact *n*-octane hydroconversion due to a preferential adsorption on the metal sites. The preferential physical adsorption of a heavier cycloalkane such as tert-butylcyclohexane in the zeolite pores only reinforced this negative impact. Correspondingly, the tendency to shift the alkane hydrocracking regime from ideal to non-ideal becomes stronger with the size difference between cycloalkane and alkane. Conversely, *n*-octane did not impact conversion and product selectivity of both methylcyclohexane and tert-butylcyclohexane.

Methylcyclohexane admixture did not impact *n*-decane conversion and products selectivity over the well-balanced catalyst. Nevertheless, over the poorly-balanced catalyst, the *n*-decane conversion was lowered by methylcyclohexane admixture. Hence, the impact of lower carbon number cycloalkane admixtures on higher carbon number *n*-alkane hydroconversion becomes less pronounced with increasing difference in carbon number. In the most extreme case, i.e., methylcyclohexane admixture to *n*-decane on a well-balanced catalyst, the impact even totally disappeared. In such a case, the preferential adsorption of the lower carbon number cycloalkane on the metal sites does not suffice to shift the hydrocracking of the higher carbon number alkane, preferentially physisorbing in the zeolite pores, from ideal to nonideal. The preferential physisorption of *n*-decane causes lower conversion of methylcyclohexane in mixture.

## *Associated content*

**Supporting Information:** The Supporting Information is available free of charge.

Temperature profile of the calcination program; Catalyst characterization – t-plot data, ICP-OES data, Hydrogen temperature programmed reduction, Hydrogen-oxygen titration data, Transmission electron microscopy (TEM), Ammonia temperature programmed desorption; Determination of metal-acid sites ratio; Verification of the mass and heat transfer limitations in the performed experiments; Generic and physisorption properties of model components; Reaction network characteristics of model components; Qualitative analysis of products of tert-butylcyclohexane hydroconversion; *n*-Octane conversion, when fed pure and in 1:1 n/n mixture with methylcyclohexane and with tert-butylcyclohexane, at various conditions as a function of space time calculated based on *n*-octane flow rate over 0.3 wt%Pt/HUSY and 0.07 wt%Pt/HUSY; Magnified Figure 6 *n*-octane isomer yields as a function of *n*-octane conversion, when fed pure and in 1:1 n/n mixture with methylcyclohexane and with tert-butylcyclohexane over 0.3 wt%Pt/HUSY and 0.07 wt%Pt/HUSY; tert-butylcyclohexane conversion, when fed pure and in 1:1 n/n mixture with *n*-octane, at various conditions as a function of space time calculated based on tert-butylcyclohexane flow rate over 0.3 wt%Pt/HUSY and 0.07 wt%Pt/HUSY; Conversion of *n*-decane when fed

pure and in 1:1 n/n mixture with methylcyclohexane, at various conditions as a function of space time calculated based on *n*-decane flow rate; Methylcyclohexane conversion, when fed pure and in 1:1 n/n mixture with *n*-decane, at various conditions as a function of space time calculated based on methylcyclohexane flow rate over 0.3 wt%Pt/HUSY and 0.07 wt%Pt/HUSY.

**Data availability statement:** The kinetic measurements on hydrocracking which are presented in the article can be found in attachment (Zenodo data base). The characterization data ($H_2$-$O_2$ titration and $N_2$ adsorption) of catalysts can be found in attachment (Zenodo data base).

## *Author contribution statement*

**Nebojsa Korica**: Investigation, Conceptualization, Methodology, Validation, Visualization, Data Curation, Writing – Original Draft; **Arij Ben Hassine:** Investigation, Visualization; **Hang Dao Thi:** Investigation, Resources, Writing – Review & Editing; **Latifa Bergaoui:** Supervision; **Kevin M. Van Geem:** Resources, Writing – Review & Editing; **Pedro S.F. Mendes**: Conceptualization, Supervision, Methodology, Writing – Review & Editing; **Jeriffa De Clercq**: Conceptualization, Supervision, Writing – Review & Editing, Funding acquisition; **Joris W. Thybaut**: Conceptualization, Supervision, Resources, Writing – Review & Editing, Funding acquisition.

## *Author information*

**Corresponding Author**

**Joris W. Thybaut:** Laboratory for Chemical Technology, Ghent University, Technologiepark 125, B-9052 Ghent, Belgium

E-mail : Joris.Thybaut@ugent.be

**Authors**

**Nebojsa Korica**: Laboratory for Chemical Technology, Ghent University, Technologiepark 125, B-9052 Ghent, Belgium

**Arij Ben Hassine:** National Institute of Applied Science and Technology (INSAT), Centre Urbain Nord BP 676, 1080 Tunis Cedex, Tunisia

**Hang Dao Thi:** Laboratory for Chemical Technology, Ghent University, Technologiepark 125, B-9052 Ghent, Belgium

**Latifa Bergaoui:** National Institute of Applied Science and Technology (INSAT), Centre Urbain Nord BP 676, 1080 Tunis Cedex, Tunisia

**Kevin Van Geem:** Laboratory for Chemical Technology, Ghent University, Technologiepark 125, B-9052 Ghent, Belgium

**Pedro S.F. Mendes**: Laboratory for Chemical Technology, Ghent University, Technologiepark 125, B-9052 Ghent, Belgium (present address Centro de Química Estrutural, Instituto Superior Técnico, Universidade de Lisboa, Av. Rovisco Pais, 1049-001 Lisbon, Portugal)

**Jeriffa De Clercq:** Industrial Adsorption and Catalysis Technology, Ghent University, Valentin Vaerwyckweg 1, B-9000 Ghent, Belgium

**Notes**

The authors declare no competing financial interest.

## *Acknowledgements*

This work has been supported by funding from the European Research Council under the European Union's Seventh Framework Programme (FP7/2007-2013) / ERC grant agreement No 615456, and by funding from the European Union's Horizon 2020 research and innovation programme under grant agreement No 964007.

Pedro S. F. Mendes acknowledges the financial support of the Special Research Fund of Ghent University for the post-doctoral assistant research mandate (BOF/PDO/2018/001901).

## *References*

1. Scherzer, J. G., A.J., *Hydrocracking Science and Technology*. 1st Edition ed.; Marcel Dekker: New York, 1996.

2. Meusinger, J., Hydrocracking Science and Technology. J. A. SCHERZER, A. J. GRUIA. Marcel Dekker, New York, 1996, 320 Seiten, Zahlr. Abb. u. Tab., geb., $ 165,–, ISBN 0-8247-9760-4. *Chemie Ingenieur Technik* **1997,** 69, (8), 1161-1162.
3. Ward, J. W., Hydrocracking processes and catalysts. *Fuel Processing Technology* **1993,** 35, (1), 55-85.
4. Weitkamp, J., Catalytic Hydrocracking—Mechanisms and Versatility of the Process. *ChemCatChem* **2012,** 4, (3), 292-306.
5. Coonradt, H. L.; Garwood, W. E., Mechanism of Hydrocracking Reaction of Paraffins and Olefins *Industrial & Engineering Chemistry Process Design and Development* **1964,** 3, (1), 38-45.
6. Degnan, T. F.; Kennedy, C. R., Impact of Catalyst Acid/Metal Balance in Hydroisomerization of Normal Paraffins. *AlChE Journal* **1993,** 39, (4), 607-614.
7. Alvarez, F.; Ribeiro, F. R.; Perot, G.; Thomazeau, C.; Guisnet, M., Hydroisomerization and Hydrocracking of Alkanes: 7. Influence of the Balance between Acid and Hydrogenating Functions on the Transformation ofn-Decane on PtHY Catalysts. *Journal of Catalysis* **1996,** 162, (2), 179-189.
8. Martens, J. A.; Tielen, M.; Jacobs, P. A., Attempts to rationalize the distribution of hydrocracked products. III. mechanistic aspects of isomerization and hydrocracking of branched alkanes on ideal bifunctional large-pore zeolite catalysts. *Catalysis Today* **1987,** 1, (4), 435-453.
9. Baltanás, M. A.; Vansina, H.; Froment, G. F., Hydroisomerization and Hydrocracking. 5. Kinetic - Analysis of Rate Data for n-octane. *Industrial & Engineering Chemistry Product Research and Development* **1983,** 22, (4), 531-539.
10. Thybaut, J. W.; Marin, G. B.; Baron, G. V.; Jacobs, P. A.; Martens, J. A., Alkene Protonation Enthalpy Determination from Fundamental Kinetic Modeling of Alkane Hydroconversion on Pt/H–(US)Y-Zeolite. *Journal of Catalysis* **2001,** 202, (2), 324-339.
11. Thybaut, J. W.; Narasimhan, C. S. L.; Marin, G. B.; Denayer, J. F. M.; Baron, G. V.; Jacobs, P. A.; Martens, J. A., Alkylcarbenium Ion Concentrations in Zeolite Pores During Octane Hydrocracking on Pt/H-USY Zeolite. *Catalysis Letters* **2004,** 94, (1), 81-88.
12. Martens, G. G.; Marin, G. B.; Martens, J. A.; Jacobs, P. A.; Baron, G. V., A Fundamental Kinetic Model for Hydrocracking of C8 to C12 Alkanes on Pt/US–Y Zeolites. *Journal of Catalysis* **2000,** 195, (2), 253-267.
13. Martens, G. G.; Thybaut, J. W.; Marin, G. B., Single-Event Rate Parameters for the Hydrocracking of Cycloalkanes on Pt/US-Y Zeolites. *Industrial & Engineering Chemistry Research* **2001,** 40, (8), 1832-1844.
14. Surla, K.; Guillaume, D.; Verstraete, J. J.; Galtier, P., Kinetic Modeling using the Single-Event Methodology: Application to the Isomerization of Light Paraffins. *Oil Gas Sci. Technol. – Rev. IFP Energies nouvelles* **2011,** 66, (3), 343-365.
15. Thybaut, J. W.; Marin, G. B., Single-Event MicroKinetics: Catalyst design for complex reaction networks. *Journal of Catalysis* **2013,** 308, 352-362.
16. Korica, N.; Mendes, P. S. F.; De Clercq, J.; Thybaut, J. W., Interplay of Metal-Acid Balance and Methylcyclohexane Admixture Effect on n-Octane Hydroconversion over Pt/HUSY. *Industrial & Engineering Chemistry Research* **2021,** 60, (34), 12505-12520.
17. Guisnet, M., "Ideal" bifunctional catalysis over Pt-acid zeolites. *Catalysis Today* **2013,** 218-219, 123-134.
18. Batalha, N.; Pinard, L.; Bouchy, C.; Guillon, E.; Guisnet, M., n-Hexadecane hydroisomerization over Pt-HBEA catalysts. Quantification and effect of the intimacy between metal and protonic sites. *Journal of Catalysis* **2013,** 307, 122-131.
19. Oenema, J.; Harmel, J.; Vélez, R. P.; Meijerink, M. J.; Eijsvogel, W.; Poursaeidesfahani, A.; Vlugt, T. J. H.; Zečević, J.; de Jong, K. P., Influence of Nanoscale Intimacy and Zeolite Micropore Size on the Performance of Bifunctional Catalysts for n-Heptane Hydroisomerization. *ACS Catalysis* **2020,** 10, (23), 14245-14257.

20. Zecevic, J.; Vanbutsele, G.; de Jong, K. P.; Martens, J. A., Nanoscale intimacy in bifunctional catalysts for selective conversion of hydrocarbons. *Nature* **2015,** 528, 245.
21. Mendes, P. S. F.; Silva, J. M.; Ribeiro, M. F.; Daudin, A.; Bouchy, C., From powder to extrudate zeolite-based bifunctional hydroisomerization catalysts: on preserving zeolite integrity and optimizing Pt location. *Journal of Industrial and Engineering Chemistry* **2018,** 62, 72-83.
22. Mendes, P. S. F.; Silva, J. M.; Ribeiro, M. F.; Daudin, A.; Bouchy, C., Bifunctional Intimacy and its Interplay with Metal-Acid Balance in Shaped Hydroisomerization Catalysts. *ChemCatChem* **2020,** 12, (18), 4582-4592.
23. Gutierrez-Acebo, E.; Leroux, C.; Chizallet, C.; Schuurman, Y.; Bouchy, C., Metal/Acid Bifunctional Catalysis and Intimacy Criterion for Ethylcyclohexane Hydroconversion: When Proximity Does Not Matter. *ACS Catalysis* **2018,** 8, (7), 6035-6046.
24. Thybaut, J. W.; Laxmi Narasimhan, C. S.; Denayer, J. F.; Baron, G. V.; Jacobs, P. A.; Martens, J. A.; Marin, G. B., Acid−Metal Balance of a Hydrocracking Catalyst: Ideal versus Nonideal Behavior. *Industrial & Engineering Chemistry Research* **2005,** 44, (14), 5159-5169.
25. Sánchez, P.; Dorado, F.; Ramos, M. J.; Romero, R.; Jiménez, V.; Valverde, J. L., Hydroisomerization of C6–C8 n-alkanes, cyclohexane and benzene over palladium and platinum beta catalysts agglomerated with bentonite. *Applied Catalysis A: General* **2006,** 314, (2), 248-255.
26. Jiménez, C.; Romero, F. J.; Roldán, R.; Marinas, J. M.; Gómez, J. P., Hydroisomerization of a hydrocarbon feed containing n-hexane, n-heptane and cyclohexane on zeolite-supported platinum catalysts. *Applied Catalysis A: General* **2003,** 249, (1), 175-185.
27. Roldán, R.; Romero, F. J.; Jiménez-Sanchidrián, C.; Marinas, J. M.; Gómez, J. P., Influence of acidity and pore geometry on the product distribution in the hydroisomerization of light paraffins on zeolites. *Applied Catalysis A: General* **2005,** 288, (1), 104-115.
28. Holló, A.; Hancsók, J.; Kalló, D., Kinetics of hydroisomerization of C5–C7 alkanes and their mixtures over platinum containing mordenite. *Applied Catalysis A: General* **2002,** 229, (1), 93-102.
29. Guisnet, M.; Fouche, V., Isomerization of n-hexane on platinum dealuminated mordenite catalysts III. Influence of hydrocarbon impurities. *Applied Catalysis* **1991,** 71, (2), 307-317.
30. Denayer, J. F. M.; Baron, G. V., Adsorption of normal and branched paraffins in faujasite zeolites NaY, HY, Pt/NaY and USY. *Adsorption* **1997,** 3, (4), 251-265.
31. Denayer, J. F.; Baron, G. V.; Martens, J. A.; Jacobs, P. A., Chromatographic Study of Adsorption of n-Alkanes on Zeolites at High Temperatures. *The Journal of Physical Chemistry B* **1998,** 102, (17), 3077-3081.
32. Denayer, J. F.; Baron, G. V.; Jacobs, P. A.; Martens, J. A., Competitive physisorption effects in hydroisomerisation of n-alkane mixtures on Pt/Y and Pt/USY zeolite catalysts. *Physical Chemistry Chemical Physics* **2000,** 2, (5), 1007-1014.
33. Denayer, J. F. M.; Martens, J. A.; Jacobs, P. A.; Thybaut, J. W.; Marin, G. B.; Baron, G. V., Influence of the zeolite composition on the hydro-isomerisation and hydrocracking of alkanes on Pt/USY zeolites: modelling of the reaction kinetics using an adsorption–reaction approach. *Applied Catalysis A: General* **2003,** 246, (1), 17-28.
34. Monteiro, C. A. A.; Costa, D.; Zotin, J. L.; Cardoso, D., Effect of metal–acid site balance on hydroconversion of decalin over Pt/Beta zeolite bifunctional catalysts. *Fuel* **2015,** 160, 71-79.
35. Mendes, P. S. F.; Silva, J. M.; Ribeiro, F. R.; Duchene, P.; Daudin, A.; Bouchy, C., Quantification of Metal-Acid Balance in Hydroisomerization Catalysts: A Step Further Toward Catalyst Design. *AlChE Journal* **2017,** 63, (7), 2864-2875.
36. Mendes, P. S. F.; Lapisardi, G.; Bouchy, C.; Rivallan, M.; Silva, J. M.; Ribeiro, M. F., Hydrogenating activity of Pt/zeolite catalysts focusing acid support and metal dispersion influence. *Applied Catalysis A: General* **2015,** 504, 17-28.

37. Bartholemew, C. H., H2 adsorption on supported noble metals and its use in determining metal dispersion. In *Catalysis: Volume 11*, Spivey, J. J.; Agarwal, S. K., Eds. The Royal Society of Chemistry: 1994; Vol. 11, pp 93-126.
38. Prasad, J.; Murthy, K. R.; Menon, P. G., The stoichiometry of hydrogen-oxygen titrations on supported platinum catalysts. *Journal of Catalysis* **1978,** 52, (3), 515-520.
39. Morin, S.; Ayrault, P.; Gnep, N. S.; Guisnet, M., Influence of the framework composition of commerical HFAU zeolites on their activity and selectivity in m-xylene transformation. *Applied Catalysis A: General* **1998,** 166, (2), 281-292.
40. Neves, I. C.; Botelho, G.; Machado, A. V.; Rebelo, P., Catalytic degradation of polyethylene: An evaluation of the effect of dealuminated Y zeolites using thermal analysis. *Materials Chemistry and Physics* **2007,** 104, (1), 5-9.
41. Remy, M. J.; Stanica, D.; Poncelet, G.; Feijen, E. J. P.; Grobet, P. J.; Martens, J. A.; Jacobs, P. A., Dealuminated H−Y Zeolites: Relation between Physicochemical Properties and Catalytic Activity in Heptane and Decane Isomerization. *The Journal of Physical Chemistry* **1996,** 100, (30), 12440-12447.
42. Mendes, P. S. F.; Taleb, A.-L.; Gay, A.-S.; Daudin, A.; Bouchy, C.; Silva, J. M.; Ribeiro, M. F., Nanoscale insights into Pt-impregnated mixtures of zeolites. *Journal of Materials Chemistry A* **2017,** 5, (32), 16822-16833.
43. Borght, K.; Toch, K.; Galvita, V.; Thybaut, J.; Marin, G., Information-Driven Catalyst Design Based on High-Throughput Intrinsic Kinetics. *Catalysts* **2015,** 5, (4), 1948-1968.
44. Dao Thi, H.; Djokic, M. R.; Van Geem, K. M., Detailed Group-Type Characterization of Plastic-Waste Pyrolysis Oils: By Comprehensive Two-Dimensional Gas Chromatography Including Linear, Branched, and Di-Olefins. *Separations* **2021,** 8, (7).
45. Ristic, N. D.; Djokic, M. R.; Konist, A.; Van Geem, K. M.; Marin, G. B., Quantitative compositional analysis of Estonian shale oil using comprehensive two dimensional gas chromatography. *Fuel Processing Technology* **2017,** 167, 241-249.
46. Berger, R. J. *EUROKIN spreadsheet on requirements for measurement of intrinsic kinetics in the gas-solid fixed-bed reactor*, EUROKIN consortium: 2012.
47. Dietz, W. A., Response Factors for Gas Chromatographic Analyses. *Journal of Chromatographic Science* **1967,** 5, (2), 68-71.
48. Denayer, J. F.; Souverijns, W.; Jacobs, P. A.; Martens, J. A.; Baron, G. V., High-Temperature Low-Pressure Adsorption of Branched C5−C8 Alkanes on Zeolite Beta, ZSM-5, ZSM-22, Zeolite Y, and Mordenite. *The Journal of Physical Chemistry B* **1998,** 102, (23), 4588-4597.
49. Kriz, J. F.; Pope, T. D.; Stanciulescu, M.; Monnier, J., Catalysts for the Isomerization of C7 Paraffins. *Industrial & Engineering Chemistry Research* **1998,** 37, (12), 4560-4569.
50. Denayer, J. F.; Baron, G. V.; Vanbutsele, G.; Jacobs, P. A.; Martens, J. A., Evidence for Alkylcarbenium Ion Reaction Intermediates from Intrinsic Reaction Kinetics of C6–C9n-Alkane Hydroisomerization and Hydrocracking on Pt/H–Y and Pt/USY Zeolites. *Journal of Catalysis* **2000,** 190, (2), 469-473.